ON-LINE APPENDIX

Methods: Automated Brain Segmentation

CTSeg adapts the unified segmentation algorithm[1] from the SPM Toolbox, Version 12.[2] SPM is widely used for segmenting brain tissues such as the GM, WM, CSF, and skull from MR images. SPM creates probabilistic tissue maps for each tissue type, and these maps describe the probability of each voxel belonging to a certain tissue. SPM segments the brain tissues by iteratively modeling the intensity distribution of each tissue type to derive posterior tissue probabilities using the Bayes rule followed by spatial normalization of the standard tissue probability map (TPM)[3] to the obtained posterior probabilistic map, and it updates the priors to be used in the next iteration. This method is independent of the absolute tissue intensity in the original image—that is, the intensity distributions are modeled for each image independently, making this method easily adaptable for segmentation of brain images from different modalities that have different intensities for the tissues. CT images differ from MR images in both the range of tissue intensity and the contrast-to-noise ratio between tissue types. In this work, we adapt SPM segmentation to model CT image intensities.

The first step in SPM segmentation is to perform an initial registration of the native space MR image, to be segmented, onto an International Consortium for Brain Mapping (ICBM; http://www.bmap.ucla.edu/portfolio/atlases/ICBM_Template/) MR brain template[3] in the Montreal Neurological Institute space. The registered image iteratively goes through tissue classification, bias-correction, and spatial normalization until all the parameters are optimized to construct the final partial tissue volume maps.[1] The initial registration of the native space image is the only step that is specific to an MR image because the template used is an MR imaging template. We adapted this method for our CTSeg pipeline to perform CT image segmentation using a CT template that was registered to the TPM or the ICBM MR imaging template needed for the initial affine registration step. Using an adult CT brain template developed by Rorden et al,[4] we aligned the CT image to the TPM in the Montreal Neurological Institute space. In the process of creating the CT template, Rorden et al used an intensity transformation for the CT images for better registration with the MR image template. The CT template thus created was in the new intensity space; therefore, an initial step was required to transform the CT image intensities before proceeding with the registration. The TPM used here during segmentation was created originally for MR images. However, the TPM contains only voxel-wise tissue probabilities and is independent of the imaging modality. Therefore, we used the default TPM provided in SPM for the CTSeg pipeline.

The de-identified CT images of the patients were obtained i n DICOM format and converted into the Neuroimaging Informatics and Technology Initiative (NIfTI; https://nifti.nimh.nih.gov/) format using dcm2niix[5] software provided with MRIcroGL, Version 2016 (http://www.mccauslandcenter.sc.edu/mricrogl/).

The CTSeg pipeline is outlined in Fig 1, and the steps involved in the pipeline are described below:

1. Intensity transformation: CT image voxel intensities (in Hounsfield units) are transformed to the Cormack units using the method outlined in Rorden et al[4] (https://github.com/neurolabusc/Clinical/blob/master/clinical_h2c.m) to match the intensity space of the CT template.
2. Registration: The transformed image is then spatially registered to the CT template using a 12-parameter affine registration using FMRIB Linear Image Registration Tool (FLIRT; http://www.fmrib.ox.ac.uk/fsl/fslwiki/FLIRT).[6,7] The affine matrix obtained during the registration is retained for use in step 5.
3. SPM segmentation: The registered CT image is segmented using SPM, with default parameters, to create tissue probability maps for GM, WM, and CSF. The affine regularization option is selected as "no affine registration" because we already registered the CT image to the Montreal Neurological Institute space template in Step 2.
4. Adding probabilistic maps: GM and WM maps are added to obtain a probabilistic map for the brain parenchyma; GM, WM, and CSF maps are added to obtain the probabilistic map of the intracranial space.
5. Affine transformation to native space: The probabilistic segmentation maps of the brain and intracranial space are transformed back to the native space of the original CT image using the inverse of the affine registration matrix computed in step 2.
6. Binarization: The probabilistic maps of the intracranial space and brain parenchyma in the native space are binarized by thresholding using respective optimal threshold values to create binary segmentation maps. Selection of optimal threshold is discussed in the next section.

Although CTSeg creates individual GM and WM maps, we summed them to obtain brain parenchymal maps to obtain TBV. Moreover, the validity of individual GM and WM maps derived through the above process is questionable due to the low contrast-to-noise ratio among the tissues in CT. Although several previous studies used GM and WM probabilistic maps obtained from CT images,[8,9] they did not systematically establish the validity of the GM and WM maps using ground truth segmentations.

Optimal Threshold Selection

The probabilistic maps of the brain and the intracranial space obtained by applying CTSeg were binarized by thresholding them to obtain the respective binary masks and were compared with their respective manual segmentation masks using Dice similarity index (DSI).[10] DSI was calculated using the following formula:

$$SI = \frac{2 \times TP}{2 \times TP + FN + FP},$$

where TP refers to the true-positive voxels where both the binary mask voxels and the corresponding ground truth voxels (from manual segmentation) indicated the tissue presence. FP refers to false-positive voxels where the binary mask indicated

the tissue presence when there was no tissue in ground truth. *FN* refers to the number of false-negative voxels where the binary mask indicated no tissue while the ground truth indicated the tissue presence. For both brain and intracranial probabilistic maps, DSI was computed for a range of probability threshold values between 0 and 1 on the training dataset (subset of the manual dataset) and was tested on the rest of the images. The optimal threshold was selected using the following procedure for brain and intracranial space maps independently: A set of 10 images from the manual dataset was randomly selected as the training set with the remaining 10 used for testing. All the voxels from images in the training set were pooled into a single array, separately for the probabilistic map and the manual segmentation mask. The optimal threshold was identified using a random search between 0 and 1 as the threshold value that exhibited the highest DSI on the pooled array of voxels. The optimal threshold was then applied to binarize the probabilistic maps of the test images, and DSI was computed for each test image individually. The robustness of the optimal thresholds was also verified using leave-one-out cross-validation.

The DSI calculated by applying the above optimal thresholds on the test images was 0.94 ± 0.008 for the brain mask and 0.98 ± 0.002 for the intracranial mask (On-line Fig 1). When the above optimal thresholds were individually applied on the training images, we obtained a DSI of 0.95 ± 0.012 for the brain mask and 0.98 ± 0.003 for the intracranial mask. Similarity of the DSIs on both testing and training datasets show that the above-selected optimal thresholds are robust. The robustness of the binarization was also verified using leave-one-out cross-validation. The optimal threshold with the leave-one-out cross-validation was close to the optimal threshold obtained in the first approach.

REFERENCES

1. Ashburner J, Friston KJ. **Unified segmentation.** *Neuroimage* 2005; 26:839–51 CrossRef Medline
2. Tzourio-Mazoyer N, Landeau B, Papathanassiou D, et al. **Automated anatomical labeling of activations in SPM using a macroscopic anatomical parcellation of the MNI MRI single-subject brain.** *Neuroimage* 2002;15:273–89 CrossRef Medline
3. Mazziotta J, Toga A, Evans A, et al. **A probabilistic atlas and reference system for the human brain: International Consortium for Brain Mapping (ICBM).** *Philos Trans R Soc London Ser B* 2001;356:1293–322 CrossRef Medline
4. Rorden C, Bonilha L, Fridriksson J, et al. **Age-specific CT and MRI templates for spatial normalization.** *Neuroimage* 2012;61:957–65 CrossRef
5. Li X, Morgan PS, Ashburner J, et al. **The first step for neuroimaging data analysis: DICOM to NIfTI conversion.** *J Neurosci Methods* 2016;264:47–56 CrossRef Medline
6. Jenkinson M, Smith S. **A global optimisation method for robust affine registration of brain images.** *Med Image Anal* 2001;5:143–56 CrossRef Medline
7. Jenkinson M, Pechaud M, Smith S. **BET2: MR-based estimation of brain, skull and scalp surfaces.** http://mickaelpechaud.free.fr/these/HBM05.pdf. Accessed May 13, 2019
8. Imabayashi E, Matsuda H, Tabira T, et al. **Comparison between brain CT and MRI for voxel-based morphometry of Alzheimer's disease.** *Brain Behav* 2013;3:487–93 CrossRef Medline
9. Kemmling A, Wersching H, Berger K, et al. **Decomposing the Hounsfield unit: probabilistic segmentation of brain tissue in computed tomography.** *Clin Neuroradiol* 2012;22:79–91 CrossRef
10. Dice LR. **Measures of the amount of ecologic association between species.** *Ecology* 1945;26:297–302 CrossRef

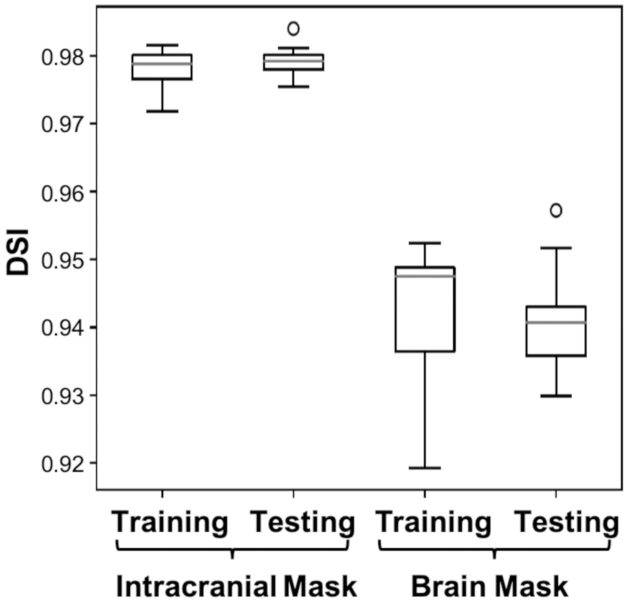

ON-LINE FIG 1. Dice similarity index (DSI) computed for brain and intracranial binary masks of the test subjects.

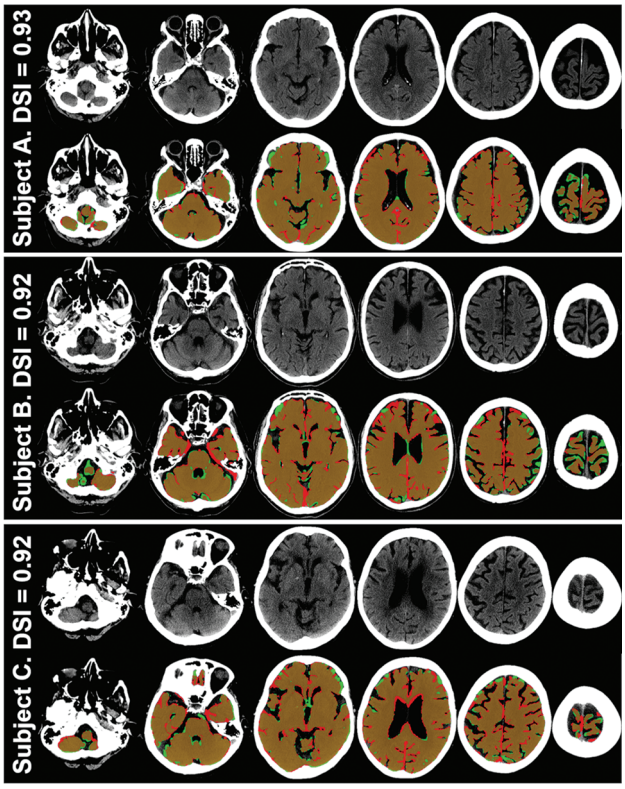

ON-LINE FIG 2. Axial views of head CT slices for the 3 subjects who showed the highest TBV error. *Upper row* of each subject is the original CT image viewed in the brain intensity window (40–80 HU), and the second row is the binary brain mask of CTSeg overlaid on the manual segmentation mask and the original CT image slices. Brown represents regions where CTSeg and the manual segmentations agree. *Red regions* represent false-positive labeling by CTSeg, and *green regions* represent the false-negatives. DSI indicates the Dice similarity index.

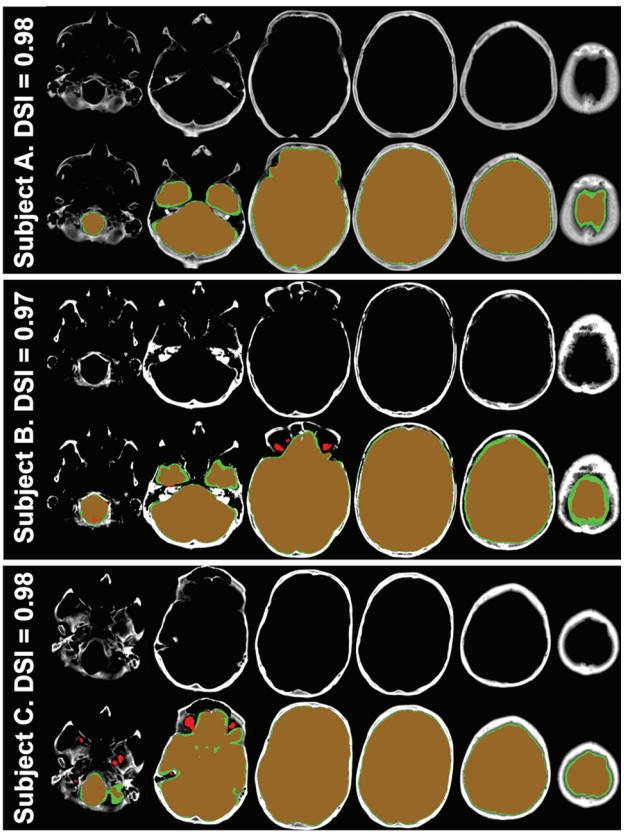

ON-LINE FIG 3. Axial views of head CT images for the 3 subjects who showed the highest TIV error. *Upper row* of each subject is the original CT image viewed in the bone intensity window (300–1500 HU), and second row is the binary intracranial mask from CTSeg overlaid on the manual segmentation mask and the original CT image. *Brown regions* represent the voxels where the CTSeg and manual segmentations agree. *Red regions* represent false-positive labeling by CTSeg, and *green regions* represent the false-negatives. DSI indicates the Dice similarity index.

On-line Table 1: Scanner and image parameters[a]

Manual Segmentation Dataset ($n = 20$)	AD Dataset ($n = 152$)	
	AD ($n = 62$)	Controls ($n = 90$)
Scanner Model		
LightSpeed VCT (12)[b]	LightSpeed VCT (26)	LightSpeed VCT (42)
LightSpeed 16 (4)[b]	LightSpeed 16 (18)	LightSpeed 16 (19)
Aquilion (4)[c]	Sensation 64 (1)[d]	Sensation 64 (1)
	Aquilion (17)	Sensation 16 (2)[d]
		Aquilion (26)
Section Thickness (mm)		
5.0	5.0	5.0
Pixel size (mm)		
0.4 × 0.4 (2)	0.4 × 0.4 (5)	0.4 × 0.4 (3)
0.5 × 0.5 (18)	0.5 × 0.5 (57)	0.5 × 0.5 (87)

[a] Number of images are indicated in parentheses.
[b] GE Healthcare, Milwaukee, Wisconsin.
[c] Toshiba Medical Systems, Tokyo, Japan.
[d] Siemens, Erlangen, Germany.

On-line Table 2: Results of linear regression analysis

Model	Dependent Variable	Included Predictor	B	Standard Error of B	*P* Value
1	%TBV	Intercept	99.61		
		Age	–0.28	0.06	<.0001
		AD diagnosis	–1.28	0.51	.014
2	%TBV	Intercept	93.02		
		Age	–0.20	0.09	.03
		AD diagnosis	12.30	9.94	.21
		Age × AD diagnosis	–0.17	0.13	.17
3	TBV	Intercept	0.29		
		Age	–0.004	0.001	<.0001
		Sex	–0.001	0.009	.90
		TIV	0.766	0.031	<.0001
		AD diagnosis	–0.017	0.007	.013
4	TBV	Intercept	0.201		
		Age	–0.002	0.001	.054
		Sex	–0.0004	0.009	.965
		TIV	–0.76	0.031	<.0001
		AD diagnosis	0.178	0.133	.186
		Age × AD diagnosis	–.0025	0.002	.146
5	TBV	Intercept	0.293		
		Age	–0.0036	0.0008	<.0001
		TIV	0.763	0.025	<.0001
		AD diagnosis	–0.017	0.007	.013

Note:—B indicates the beta coefficients of the linear regression.

On-line Table 3: Segmentation failure rates of the CTSeg pipeline for different scanners[a]

Scanner	AD	Controls	Total
LightSpeed VCT	2/26	7/42	9/68 (13%)
LightSpeed 16	1/18	3/19	4/37 (11%)
Sensation 16	0/0	0/1	0/1 (0%)
Sensation 64	0/1	0/2	0/3 (0%)
Aquilion	1/17	3/26	4/43 (10%)
Total	4/62 (6%)	13/90 (14%)	17/152 (11%)

[a] Values are N_{failed}/N_{total}; in parentheses are failure rates as a percentage.